HHS Public Access

Author manuscript

Mol Pharm. Author manuscript; available in PMC 2018 May 01.

Published in final edited form as:

Mol Pharm. 2017 May 01; 14(5): 1469–1481. doi:10.1021/acs.molpharmaceut.6b01088.

Encapsulation of an EP67-conjugated CTL peptide vaccine in nanoscale biodegradable particles increases the efficacy of respiratory immunization and affects the magnitude and memory subsets of vaccine-generated mucosal and systemic CD8+ T cells in a diameter-dependent manner

Bala V. K. Karuturi[‡,1], **Shailendra B. Tallapaka**[‡,3], **Pravin Yeapuri**[3], **Stephen M. Curran**[2], **Sam D. Sanderson**[3], and **Joseph A. Vetro**[2,3,*]

[1]Mylan Pharmaceuticals Inc., 781 Chestnut Ridge Road, Morgantown, WV 26505, USA

[2]Center for Drug Delivery and Nanomedicine, College of Pharmacy, University of Nebraska Medical Center, 986025 Nebraska Medical Center, Omaha, Nebraska 68198-6025, USA

[3]Department of Pharmaceutical Sciences, College of Pharmacy, University of Nebraska Medical Center, 986025 Nebraska Medical Center, Omaha, Nebraska 68198-6025, USA

Abstract

The diameter of biodegradable particles used to co-encapsulate immunostimulants and subunit vaccines affects the magnitude of memory CD8+ T cells generated by systemic immunization. Possible effects on the magnitude of CD8+ T cells generated by mucosal immunization or memory subsets that potentially correlate more strongly with protection against certain pathogens, however, are unknown. In this study, we conjugated our novel host-derived mucosal immunostimulant, EP67, to the protective MCMV CTL epitope, pp89, through a lysosomal protease-labile double arginine linker (pp89-RR-EP67) and encapsulated in PLGA 50:50 micro- or nanoparticles. We then compared total magnitude, effector/central memory (CD127/KRLG1/CD62L), and IFN-γ/TNF-α/IL-2 secreting subsets of pp89-specific CD8+ T cells as well as protection of naïve female BALB/c mice against primary respiratory infection with MCMV 21 days after respiratory immunization. We found that decreasing the diameter of encapsulating particle from ~5.4 μm to ~350 nm: (i.) increased the magnitude of pp89-specific CD8+ T cells in the lungs and spleen (ii.) partially changed CD127/KLRG1 effector memory subsets in the lungs but not the spleen (iii.) changed CD127/KRLG1/CD62L effector/central memory subsets in the spleen (iv.) changed pp89-responsive IFN-γ/TNF-α/IL-2 secreting subsets in the lungs and spleen (v.) did not affect the extent to which encapsulation increased efficacy against primary MCMV respiratory infection over unencapsulated pp89-RR-EP67. Thus, although not observed under our current experimental conditions with MCMV, varying the diameter of nanoscale biodegradable particles may increase the efficacy of mucosal immunization with co-encapsulated immunostimulant/subunit vaccines

[*]**Corresponding Author**, Department of Pharmaceutical Sciences, College of Pharmacy, University of Nebraska Medical Center, 986025 Nebraska Medical Center, WSH 3026A, Omaha, Nebraska 68198-6025, USA.

[‡]These authors contributed equally.

Author Contributions

The manuscript was written through contributions of all authors. All authors have given approval to the final version of the manuscript.

against certain pathogens by selectively increasing memory subset(s) of $CD8^+$ T cells that correlate the strongest with protection.

Keywords

vaccine delivery; microparticle; nanoparticle; nanosphere; microsphere; mucosal vaccine; mucosal adjuvant; host-derived immunostimulant; correlate of protection; murine cytomegalovirus

INTRODUCTION

To be effective, prophylactic vaccines must generate long-lived protective adaptive immune responses against a given pathogen at levels that correlate with a defined clinical endpoint such as a decrease in the incidence of infectious disease in a specific population[1, 2]. Most licensed vaccines to date generate long-lived plasma B cells that secrete protective pathogen-specific antibodies at levels that correspond to protection against extracellular pathogens or pathogen-derived toxins[3–5]. Neutralizing antibodies, however, are insufficient for protection against pathogens that undergo frequent changes to their surface antigens and/or predominantly remain within host cells during their lifecycle[3]. For these pathogens, there is extensive preclinical and, to a lesser extent, clinical data that long-lived memory $CD4^+$ or $CD8^+$ T cells are required for reduction, clearance, and subsequent control of infection[1, 3, 6] although isotypes of pathogen-specific antibodies may further increase the efficacy of protective T cell memory recall responses[7]. Thus, it is likely that efficacious vaccines against antibody-resistant pathogens must additionally generate long-lived protective memory T cells.

Vaccines composed of live attenuated pathogens are the most likely to generate long-lived protective memory T cells after systemic or mucosal administration at levels that correlate with protection against the wild type pathogen[8]. Live attenuated vaccines, however, require a long time to develop, seldom produce a safe and stable vaccine, may not cross-protect against different strains of the same pathogen, have the potential for pathogenic reversion, and are not an option for pathogens that can't be grown in culture[8–10]. The limitations of live attenuated vaccines can potentially be overcome by subunit vaccines composed of proteins ("recombinant protein vaccines") or peptide epitope(s) ("synthetic peptide vaccines") identified from regions of the pathogen that generate protective adaptive immune responses[11, 12]. Most proteins and peptides, however, do not generate sufficient levels of long-lived T cells because they are rapidly cleared from the administration site, inefficiently delivered to antigen-presenting cells (APCs), and lack immune stimulating moieties from the original pathogen that activate APCs[11, 12].

Co-encapsulating appropriate immunostimulants and protective proteins or peptides (i.e., subunit vaccines) within nanoscale-sized particles composed of biodegradable polymers[13] is a promising, well-established approach to increase the generation of long-lived T cells by subunit vaccines after systemic or mucosal immunization[14]. It provides several advantages including decreased vaccine degradation and clearance, increased immunostimulation at the administration site, increased levels and duration of epitope presentation and cross-

presentation by activated APCs, and increased mucosal and systemic adaptive immune responses following mucosal administration[15–25].

The diameter of nanoscale biodegradable particles is a key dosage form parameter[26–29] that potentially affects the magnitude of $CD4^+$ and $CD8^+$ T cells as well as Th1/Th2 memory subsets of $CD4^+$ T cells generated by co-encapsulated immunostimulant/subunit vaccines after systemic immunization[30, 31]. It remains unclear, however, whether the diameter of co-encapsulating biodegradable particle affects the generation of mucosal and systemic memory T cells by co-encapsulated immunostimulants/subunit vaccines after mucosal immunization. Furthermore, memory T cells continue to be further distinguished based on the expression of cell surface markers (cell surface phenotype) or the release of one or multiple cytokines after exposure to protective epitopes (functional phenotype) that collectively relate more closely to T cell functions that are critical for vaccine efficacy such as long-term survival, recall response upon re-infection with different pathogens, and cytolytic activity[32, 33]. Differential protection against several pathogens by memory subsets of $CD4^+$ and $CD8^+$ T cells has also been reported after adoptive transfer in murine models of infectious disease[34]. Thus, it is important to determine if the diameter of encapsulating biodegradable particle potentially affects not only the magnitude of vaccine-generated T cells but also established and emerging memory T cell subsets that potentially correlate more strongly with protection against the targeted pathogen[6].

We previously developed the novel host-derived peptide immunostimulant, EP67[35], based on the last 10 amino acids of the C-terminal of human complement component 5a (C5a) that minimizes the toxic pro-inflammatory side effects of the C5a parent peptide by selectively activating APCs over neutrophils[35, 36]. Systemic immunization with vaccines composed of EP67 conjugated to peptides, intact proteins, or attenuated pathogens generates Th1-biased humoral and cellular immune responses in mice presumably, in large part, by simultaneously activating DCs and increasing subsequent processing and presentation of conjugated immunogens through the binding and activation of the C5a receptor (C5aR/CD88)[37]. We also recently found that respiratory immunization with a CTL peptide vaccine composed 1/1 (w/w) with EP67 directly conjugated to the dominant protective MCMV CTL epitope pp89 or subdominant CTL epitope M84 increases protection against respiratory infection with MCMV in BALB/c mice, indicating that EP67 can act as a mucosal adjuvant[38].

In this study, we conjugated EP67 to the C-terminal of pp89 through a lysosomal protease-labile double arginine linker (pp89-RR-EP67) and intranasally administered PBS (50 μL), PBS containing unencapsulated pp89-RR-EP67 (50 μg), or PBS containing the same dose of pp89-RR-EP67 (50 μg) encapsulated in PLGA 50:50 micro- (~5.4 μm) or nanoparticles (~350 nm) to naïve female BALB/c mice. We then compared the total magnitude, effector/central memory (CD127/KRLG1/CD62L), and IFN-γ/TNF-α/IL-2 secreting subsets of pp89-specific $CD8^+$ T cells in the lungs (mucosal) and spleen (systemic) as well as protection against primary respiratory infection with MCMV 21 days after respiratory immunization.

EXPERIMENTAL SECTION

Peptides

An MCMV CTL epitope from pp89 ($_{168}$YPHFMPTNL$_{176}$) that is protective in BALB/c mice[39] wa17s synthesized and purified alone or covalently attached to the N-terminal of EP67 (YSFKDMP[MeL]aR)[35] during solid-phase synthesis via a double-arginine (RR) linker[40] to form pp89-RR-EP67. The molecular masses of the peptides were confirmed from the protonated parent ion or multiply-charged fragment ions by ESI/TOF mass spectrometry where pp89: Mcalc = 1119.3 g, $[M + H]^+$ = 1119.2709; pp89-RR-EP67: Mcalc = 2654 g, $[M + 2H]^{2+}$ = 1327.5907, $[M + 3H]^{3+}$ = 885.7130] (Fig. S1, supplementary information).

Encapsulation of pp89-RR-EP67 in biodegradable micro- and nanoparticles

The CTL peptide vaccine (pp89-RR-EP67) was encapsulated in biodegradable microparticles (MP) or nanoparticles (NP) at 5 wt% theoretical loading by the emulsification / solvent evaporation (ESE) method[22]. The primary water-oil emulsion (W_1/O) was formed by adding a sterile PBS (D-PBS w/o Mg^{2+} or Ca^{2+}) "water" solution containing pp89-RR-EP67 (20 mg/mL; 0.5 mL) to a dichloromethane (DCM) "oil" solution containing ester-terminated 50:50 poly D,L-lactic-co-glycolic acid (PLGA 50:50; research grade; inherent viscosity 0.38 dL/g; Lactel Pelham, AL; 100 mg / mL DCM; 2 mL) in a glass test tube (16 × 100 mm) and homogenized at 13,500 RPM for 1 min (Fisher Powergen 500 homogenizer) to form microparticles or sonicated for 30 sec at 50% amplitude (Misonix Sonicator 3000 w/ model 419 tapered microtip horn with 0.125 in. diameter tip) to form nanoparticles. The W_1/O emulsion was immediately transferred to a PVA solution (1% v/v polyvinyl alcohol [70% hydrolyzed; 30,000 −70,000 Da; Sigma-Aldrich] in dH_2O; 8 mL) in a 20-mL scintillation glass vial and sonicated or homogenized as described for the primary emulsion to form the secondary water-oil-water emulsion (W_1/O/W_2). The W_1/O/W_2 emulsion was then transferred to a larger volume of 1% v/v PVA solution (32 mL) in a 50-mL glass beaker and stirred (1000 rpm using a 2.5 cm, 3.97 g Teflon-coated, smooth stirring bar with molded-on pivot rings) for 4 h to fully remove DCM. Hardened NP and MP were pelleted (25,000 RCF or 20,000 RCF, respectively, for 15 min at 4°C) then resuspended and pelleted 3X using dH_2O (20 mL) to remove residual PVA. Washed particles were resuspended in dH_2O (10 mL) in a pre-weighed 20-mL scintillation vial, flash frozen in liquid N_2, lyophilized for 48 h, and stored at −20°in a capped vial sealed with parafilm.

pp89-RR-EP67 loading in PLGA particles

Peptide loading was determined as described with modification[41]. Particles (~10 mg) were equilibrated to r.t., added to DMSO (0.5 mL) in an 8-mL glass vial, and incubated for 1 hr on with constant shaking. A solution of 0.05 M NaOH/0.5% SDS in dH_2O (5 mL) was added to the DMSO/particle solution and the entire solution was stirred (400 RPM) in the capped vial for 1 hr. Undissolved polymer was pelleted (10,000 RCF, 10 min) and average peptide concentration in the supernatant was determined by Pierce Micro BCA assay (Thermo Scientific) with pp89-RR-EP67 as the standard and (1/10) DMSO/0.05 N NaOH (0.05% SDS) as the diluent. Average peptide loading (μg peptide / mg particles ± SD (n=3) was calculated as

$$\text{Peptide Loading}=[\text{Peptide } (\mu g/\text{mL})]_{\text{Supernatant}} \times \text{Sample volume } (5.5 \text{ mL})/\text{Particle mass } (10 \text{ mg})$$

and encapsulation efficiency (EE%) was calculated as

$$\text{EE\%}=\frac{\text{Assayed peptide mass } (\mu g)/\text{mass of particles } (10 \text{ mg})}{\text{Theoretical peptide mass } (50\mu g)/\text{mass of particles } (10 \text{ mg})} \times 100$$

Diameter and zeta potential of PLGA particles

Average hydrodynamic diameters and zeta-potentials ± SD (n=3 independent samples from the same batch) of the particles were measured in dH_2O (0.5 mg/mL) at 25°C using a ZetaSizer Nano ZA (Malvern Instruments, Malvern, UK) equipped with a He-Ne laser (λ = 633 nm) as the incident beam.

Peptide burst release from PLGA particles

PLGA particles (~10 mg) were added to a centrifuge tube (2 mL), resuspended in PBST (PBS and Tween-20 [0.05% v/v]; 1 mL), vortexed for 20 s, and incubated at 37°C (Vortemp 56 Shaking Incubator) with shaking (200 rpm/min). Supernatants (10,000 RCF, 5 min) were collected after 24 hrs, stored (−20°C), and the concentration of pp89-RR-EP67 determined as described above using PBST as the diluent. Average percent of pp89-RR-EP67 ± SD (n=3 independent samples from the same batch) released from the particles was calculated as

$$\%\text{pp89}-\text{RR}-\text{EP67 released}=\left[\frac{[\text{pp}89-\text{RR}-\text{EP}67(\mu\text{g/mL})]_{\text{Supernatant}} \times \text{Sample Volume } (1 \text{ mL})}{\frac{\text{mass pp}89-\text{RR}-\text{EP}67(\mu g)}{\text{mass of particles (mg)}} \times \text{mass of particles } (10 \text{ mg})}\right] \times 100$$

Animals

All animal procedures were approved by the University of Nebraska Medical Center Institutional Animal Care and Use Committee. Naïve mice (Female BALB/c AnNHsd [$H\text{-}2^d$ haplotype], 3 weeks old, Harlan Laboratories) were acclimatized in an ABSL-2 facility under pathogen-free conditions at least one week before experiments.

NIH/3T3 cells

NIH/3T3 cells (ATCC: CRL-1658) were incubated (37°C/10% CO_2) in Growth Media (DMEM containing glucose [4.5 g / L], sodium bicarbonate [3.7 g/L], heat-inactivated newborn calf serum [HI-NCS, 10% v/v, Thermo-Scientific HyClone New Zealand], L-glutamine [2 mM], sodium pyruvate [1 mM]. penicillin [100 U/mL], streptomycin G [100 μg/mL]) and passaged at ≤75% confluence.

Single mouse-passaged salivary gland-derived MCMV (P1-SGV)

Salivary gland-derived MCMV obtained from a single passage in mice (P1-SGV) was obtained by first injecting the Smith strain of MCMV (ATCC: VR-1399) in naïve female BALB/c mice (4–5 weeks old) by the intraperitoneal (IP) route (5×10^4 PFU in 0.2 mL

PBS, 25G needle), euthanizing by CO_2 asphyxiation/cervical dislocation two weeks after infection, then suspending isolated salivary glands in Freezing Media (DMEM containing glucose [4.5 g / L], sodium bicarbonate [3.7 g/L], HI-NCS [10% v/v], DMSO [cell culture grade, 10% v/v]). Isolated salivary glands were then homogenized (Fisher PowerGen 500: 6500 rpm, 45 to 60 sec; drive shaft was initially rinsed / wiped sequentially with DuPont broad-spectrum disinfectant / 70% ethanol / sterile PBS then with 70% ethanol / sterile PBS between treatment groups) and homogenate supernatants (840 RCF, 3 min) were stored as aliquots (0.3 mL) at −80°C. SGV titers were determined by plaque assay as described above.

MCMV titers

Titers of MCMV were determined by plaque assay[42]. NIH/3T3 cells were grown as described above in 24-well plates (18,000 cells/well in 0.6 mL Growth Media) for 2 days until ~40 to 50% confluent, infected with MCMV by replacing aspirated Growth Media (8 wells at a time) with 10-fold serial dilutions (10^2 to 10^6) of thawed MCMV extracts diluted in Infection Media (DMEM containing glucose [4.5 g / L], sodium bicarbonate [3.7 g/L], and HI-NCS [2% v/v]; 0.2 mL/well) that was pipetted down the side of each well (n=3 wells per dilution factor) and incubating the plate (37°C/10% CO_2) for 4 hrs with periodic shaking every 15 min for the first hr, then every 30 min. Overlay Media was prepared during MCMV infection by mixing an equal volume of pre-warmed (41°C for 10 min.) agarose solution (Seakem ME Agarose [1% w/v] in dH_2O) with pre-warmed (41°C for 10 min.) 2X Growth Media solution (HI-NCS [10% v/v] in 2X DMEM). After infection, Growth Media was quickly aspirated and replaced with Overlay Media (1 mL down the side of each well) one plate at a time and plates were incubated (37°C/10% CO_2) for 5 to 6 days. MCMV plaques were fixed by adding Fixing Solution (Formalin [10% w/v] in sterile D-PBS; 0.5 mL/well), tightly sealing stacked plates in a Ziploc® bag, and incubating at r.t. overnight. Fixing Solution was aspirated, agarose plugs were carefully removed with a steel spatula, and remaining agarose was removed by submerging the plates in cold water as needed. Plaques were visualized by incubating each well with Staining Solution (crystal violet [0.25% w/v] and ethanol [2% v/v] in dH_2O; 0.3 mL/well) at r.t. for up to 15 min, rinsing with the wells with cold water (2X), and allowing to air dry before counting by eye. Average MCMV plaque forming units (PFU) / mL ± SD (n=3 wells) was calculated as

$$\frac{\mathrm{MCMV\ \ PFU}}{\mathrm{mL}} = \mathrm{number\ \ of\ \ plaques} \times \mathrm{DF} \times \frac{1}{\mathrm{infection\ \ volume}\ (0.2\ \mathrm{mL})}$$

where *number of plaques* was taken from the organ homogenate dilution factor where 5 to 50 plaques were observed, *DF* was the selected dilution factor of the organ homogenate where 5 to 50 plaques were observed, and *infection volume* was the volume used to infect NIH/3T3 (0.2 mL). MCMV PFU / g tissue was then calculated from MCMV PFU / mL as

$$\frac{\mathrm{MCMV\ \ PFU}}{\mathrm{g\ \ tissue}} = \frac{\mathrm{MCMV\ \ PFU}}{\mathrm{mL}} \times \mathrm{extraction\ \ volume\ (mL)} \times \frac{1}{\mathrm{mass\ \ of\ \ tropic\ \ organ}\ (g)}$$

where *extraction volume* was the volume of Freezing Media used for MCMV extraction (1 mL for lungs, spleen, and salivary glands; 2 mL for liver) and *mass of tropic organ* was the

mass of the isolated organ used in the extraction. Average MCMV PFU /g ± SD (n=5 mice) were compared to PBS by one-way ANOVA with uncorrected Fisher's LSD test. Plaque assays were repeated at least once to confirm the reproducibility of the results.

Respiratory immunization

Sterile PBS alone (50 μL) or sterile PBS containing pp89-RR-EP67 alone (50 μg) or pp89-RR-EP67 (50 μg equivalent) encapsulated in MP or NP on days 0 and 7 was administered IN to naïve female BALB/c mice (4-weeks old; n=4) by anesthetizing with isoflurane in a drop jar, holding upright, and alternating drops between nares with a 200 μL pipette. Intranasal administration of 50 μL is expected to deposit vaccine primarily in the nasal cavity and lungs (i.e. respiratory immunization)[43].

Preparation of lymphocytes (lungs) and splenocytes

Mice were sacrificed by CO_2 asphyxiation/cervical dislocation on the same day as primary respiratory challenge with P1-SGV (21 days post-immunization). The lungs were then perfused by injecting ice-cold sterile D-PBS (5 mL, 25G needle) through the right ventricle of the heart and both the lungs and spleen were isolated and immediately stored on ice in sterile 15-mL conical tubes containing 5 mL of ice-cold complete RPMI Media (cRPMI: RPMI 1640 containing heat-inactivated FBS [10% v/v; < 0.3 EU endotoxin], PEN [100 U/mL]/STREP [100 μg/mL], NEAA [1% w/v], Vitamins [1% w/v], Sodium Pyruvate [1% w/v], β-mercaptoethanol [50 μM added fresh on the day of isolation]).

To isolate lymphocytes, lungs were transferred into a sterile 6-well cell culture plate (one lung/well), minced into small pieces with a sterile scalpel (#15, Bard-Parker), and incubated in cRPMI (6 mL) containing Collagenase IV (2 mg/mL; Worthington Enzymes) at 37°C for 1 hr with shaking (Vortemp 56 shaking incubator, 200 RPM). Digested lungs were triturated by pipetting (18G needle) (3X) and filtered through a sterile 70-μm cell strainer into a sterile 15-mL conical tube. Filtered cells were pelleted (400 RCF, 4°C, 5 min.), resuspended in RPMI 1460 (5 mL), layered onto Lympholyte-M (Cedarlane Labs; 5 mL) in a sterile 15-mL conical tube using a sterile Pasteur pipette, and centrifuged (1500 RCF w/o brakes, 4°C, 20 min). Lymphocytes were collected from the interphase with a sterile Pasteur pipette, transferred to a sterile 15-mL conical tube, resuspended in sterile D-PBS (10 mL), pelleted (500 RCF, 4°C, 5 min.), resuspended in cRPMI (1 mL), and stored on ice for later use.

To isolate splenocytes, spleens were transferred to a sterile 70-μm strainer inserted into a sterile 50-mL conical tube, cut into at least 3 to 4 small pieces with a sterile scalpel (#15, Bard-Parker), then gently pushed through the cell strainer with the rubber end of a sterile syringe plunge while adding RPMI 1640 (30 mL). The strainer was rinsed with additional RPMI (10 mL), filtered cells were diluted to 50 mL with sterile D-PBS, pelleted (500 RCF, 4°C, 10 min), resuspended in RBC lysis buffer (ACK Lysing Buffer; 4 mL), and incubated at r.t. for 5–7 min. After incubation, cRPMI (10 mL) was added, the entire solution was triturated with a sterile 5-mL pipette to obtain a single cell suspension, and passed through a 40-μm cell strainer into a sterile 50-mL conical tube. Filtered cells were then diluted with sterile D-PBS to 50 mL and pelleted (500 RCF, 4°C, 10 min.) (2X), resuspended in cRPMI

(3 mL), cell count and viability determined by trypan blue exclusion (Cellometer Auto T4, Nexcelom Biosciences), then stored on ice for later use.

Surface phenotype subsets of epitope-specific CD8$^+$ T cells

The surface phenotype of epitope-specific CD8a$^+$ cells was determined 21 days post-immunization by flow cytometry. Lymphocytes (lungs) and splenocytes were isolated as described above, diluted in cRPMI (10^7 cells / mL), and plated in a sterile 96-well plate (0.1 mL/well; 10^6 cells). An additional single well was plated (0.1 mL) from PBS immunizations as an unstained FACS control. Cells were pelleted (400 RCF, 5°C, 5 min), resuspended in sterile PBS (0.1 mL), pelleted (400 RCF, 5°C, 5 min.), resuspended in sterile PBS (0.1 mL) containing Zombie Yellow (1 μL, BioLegend), incubated at r.t. for 15 min in the dark, then pelleted (400 RCF, 5°C, 5 min.). Potential Fc receptors were blocked by resuspending the cells in BD Stain Buffer (0.1 mL), pelleting (400 RCF, 5°C, 5 min.), resuspending in BD Stain Buffer (0.1 mL/well) containing mouse BD Fc Block (1 μg / 10^6 cells), and incubating on ice for 20 min. Cells were stained with pp89 tetramers by resuspending in BD Stain Buffer (0.1 mL), pelleting (400 RCF, 4°C, 5 min.), resuspending in BD Stain Buffer (50 μL) [unstained cells; single well] or BD Stain Buffer (50 μL) containing Alexa 680 H-2L^d pp89-tetramers (1 μg / 10^6 cells; NIH Tetramer Core Facility at Emory University, Atlanta, Georgia, USA), and incubating at r.t. in the dark for 30 min. Cells were next stained for cell surface markers by adding BD Stain Buffer (0.1 mL), pelleting the cells (400 RCF, 4°C, 5 min.), resuspending in BD Stain Buffer (50 μL) [unstained cells; single well] or BD Stain Buffer (50 μL) containing half the manufacturer's suggested amount of FITC Anti-Mouse CD8a [Clone 53–6.7] (eBioscience), PE/Cy5 Anti-Human/Mouse CD44 [Clone IM7] (BioLegend), PE Anti-Mouse CD127 [Clone A7R34] (BioLegend), APC Anti-Mouse KLRG1 [Clone 2F1] (BioLegend), BV510 Anti-Mouse CD62L [Clone MEL-14] (BioLegend), then incubating on ice in the dark for 30 min. Cells were fixed by adding BD Stain Buffer (0.15 mL), pelleting the cells (400 RCF, 4°C, 5 min.), resuspending cells in Fixation Buffer (0.1 mL/well; BioLegend), then incubating ice for 20 min. Cells were then prepared for flow cytometry by adding BD Stain Buffer (0.150 mL), pelleting the cells (500 RCF, 4°C, 5 min.), then resuspending in BD Stain Buffer (0.2 mL) (3X).

Fixed cells were analyzed on a BD LSR II flow cytometer (Becton and Dickinson, La Jolla, CA). Instrument compensation settings were adjusted using BD CompBeads (BD Biosciences) with staining antibodies. Maximum number of events (total cells from each sample) were acquired and analyzed by FlowJo software (Tree Star, Ashland, OR, USA). The lymphocyte population was gated based on FSC (A) vs. SSC (A) plots and used for subsequent analysis (at least 15,000 CD8a$^+$ cells from the lungs and at least 10,000 CD8a$^+$ cells from the spleen). Average proportions of CD8a$^+$ cells with the indicated cell surface staining ± SD (n=4 mice) were compared by ordinary one-way ANOVA with uncorrected Fisher's LSD test or by two-tailed unpaired *t*-test as indicated.

Epitope-responsive subsets of CD8$^+$ T cells

The proportion of pp89-responsive CD8a$^+$ T cells in the lungs and spleen was compared 21 days post-immunization by intracellular cytokine staining (ICS)[44]. Lymphocytes (lungs) and splenocytes were isolated as described above, resuspended in cRPMI or cRPMI containing

pp89 [1 μM] and Brefeldin A [10 μg / mL] (10^6 cells / 0.2 mL), and incubated (37°C, 5% CO_2) for 7 hours. An additional single well was plated from PBS immunizations as an unstained FACS control. Cells were stained with Zombie Yellow, incubated with BD Fc Block, then stained with FITC Anti-Mouse CD8a [Clone 53–6.] as described above. Surface-stained cells were then fixed and permeabilized by adding BD Stain Buffer (0.15 mL), pelleting the cells (400 RCF, 4°C, 5 min.), resuspending in BD CytoFix/Cytoperm Buffer (0.1 mL), then incubating on ice for 20 min. Intracellular cytokines were stained as described above with APC Anti-Mouse IFN-γ [Clone XMG-1.2] (0.06 μg / 10^6 cells; BD Biosciences), PE Anti-Mouse TNF-α [Clone MP6-XT22] (0.25 μg / 10^6 cells; BioLegend), and Pacific Blue Anti-Mouse IL-2 [Clone JES6-5H4] (0.25 μg / 10^6 cells; BioLegend) then analyzed by flow cytometry as described above. The lymphocyte population was initially gated based on FSC (A) vs. SSC (A) plots and used for subsequent analysis. Average proportions of indicated cell populations in the spleen ± SD (n=3 mice) were compared to PBS by ordinary one-way ANOVA with uncorrected Fisher's LSD test.

Respiratory challenge with salivary gland-derived MCMV

Twenty-one days after the final immunization (Day 28), a sublethal amount of P1-SGV (5×10^3 PFU) was administered in the same manner as the vaccines. Intranasal administration in 50 μL is expected to deposit virus primarily in the nasal cavity and lungs (i.e. respiratory challenge)[43]. Average MCMV PFU /g ± SD (n=5 mice) in the salivary glands of each treatment group were compared to PBS treatment by ordinary one-way ANOVA with uncorrected Fisher's LSD test as described above.

RESULTS

The diameter of encapsulating biodegradable particle affects the magnitude of mucosal and systemic memory CD8$^+$ T cells generated by respiratory immunization with an EP67-conjugated CTL peptide vaccine

A threshold proportion of circulating pathogen-specific memory T cells correlates with clinical protection against influenza, measles, tuberculosis, and varicella[3]. Preclinical studies in mice also suggest that higher proportions of memory T cells can compensate by "mass action"[45] for T cell memory pools that are less responsive to subsequent infections[46]. Thus, the magnitude of the vaccine-generated memory T cell pool is an important criterion for vaccines that must generate long-lived memory T cells.

Protection against the development of HCMV disease in heart and lung transplant recipients directly correlates with the proportion of IFN-γ$^+$ polyclonal T cells specific for the human cytomegalovirus (HCMV) immediate early (IE)-1 protein[47]. The proportion of BALB/c mice that survives lethal primary systemic challenge with murine CMV (MCMV) also directly correlates with the number of adoptively-transferred CD8$^+$ T cells specific for the H-2L^d-restricted epitope from the analogous MCMV IE-1 protein pp89 ($_{68}$YPHFMPTNL$_{76}$)[39]. Thus, pp89-specific CD8$^+$ T cells in BALB/c mice are a relevant model for determining the effect that encapsulating EP67-conjugated peptide vaccines in nanoscale formulations has on the magnitude of the CD8$^+$ T cell memory pool generated by immunization.

To determine if encapsulation and/or the diameter of encapsulating nanoscale biodegradable particle affects the magnitude of mucosal and systemic memory $CD8^+$ T cells generated by respiratory immunization with an EP67-conjugated CTL peptide vaccine, we first covalently conjugated pp89 to the N-terminal of EP67 through a lysosomal protease-labile double arginine linker (pp89-RR-EP67) during peptide synthesis. Conjugating EP67 to CTL epitopes through a double arginine linker increases the generation of epitope-specific $CD8^+$ T cells by presumably increasing the proteolytic release of CTL epitopes during endosomal trafficking within EP67-activated DCs[40]. We next intranasally administered vehicle alone (PBS), unencapsulated pp89-RR-EP67 (Free), or pp89-RR-EP67 encapsulated in ~5.4 μm PLGA 50:50 microparticles (MP) or ~350 nm PLGA 50:50 nanoparticles (NP) (Table 1) to naïve female BALB/c mice in a volume of PBS (50 μL) expected to deliver vaccine to the nasal cavity and lungs (i.e., respiratory immunization)[43]. We then compared the proportion of mucosal (lungs) and systemic (spleen) $CD8a^+CD44^{Hi}$Tet-$pp89^+$ cells in total $CD8a^+$ T cells by flow cytometry 21 days after immunization (Fig.1A) when the majority of remaining pp89-specific $CD8^+$ T cells likely represent the memory pool[48]. Cells were additionally gated for $CD44^{Hi}$ staining to include both baseline $CD8^+$ T cell precursors and immunogen-experienced pp89-specific $CD8^+$ T cells[49].

Microparticles (Fig.1, MP) and nanoparticles (Fig.1, NP) increased the proportion of $CD8a^+CD44^{Hi}$Tet-$pp89^+$ cells between 0.24% to 0.62% over unencapsulated pp89-RR-EP67 (Fig.1, Free) and vehicle alone (Fig.1, PBS) in the lungs (Fig.1B) and spleen (Fig.1C). Furthermore, NP increased the proportion of $CD8a^+CD44^{Hi}$Tet-$pp89^+$ cells to a greater extent than MP by 0.2% in the lungs (Fig.1B) and by 0.3% in the spleen (Fig.1C). Thus, encapsulating an EP67-conjugated CTL peptide vaccine in biodegradable particles between at least ~5.4 μm and ~350 nm in diameter and decreasing the diameter from ~5.4 μm to ~350 nm increases the magnitude of mucosal and systemic memory $CD8^+$ T cells generated 21 days after respiratory immunization.

The diameter of encapsulating biodegradable particle partially changes CD127/KLRG1 memory subsets of mucosal but not systemic $CD8^+$ T cells generated by respiratory immunization with an EP67-conjugated CTL peptide vaccine

Although the magnitude is a fundamental characteristic of the T cell memory pool, it does not reflect the full potential of other T cell characteristics that are important for vaccine efficacy[32]. One such critical characteristic is the ability to generate long-lived protective adaptive immune responses given that the time and frequency of pathogen exposure is unpredictable and/or asymptomatic for some pathogens.

A well-established memory subset of $CD8^+$ T cells associated with long-lived survival is based on the relative cell surface expression of CD127 (IL-7Rα) that correlates with the intracellular expression of anti-apoptotic genes mediated through IL-7 signaling and KLRG1 that correlates with replicative senescence[50, 51]. CD127/KLRG1 memory subsets include early effector cells (EEC: $CD127^-KLRG1^-$) that can give rise to long-lived memory-precursor effector cells (MPEC: $CD127^+KLRG1^-$), short-lived effector cells (SLEC: $CD127^-KLRG1^+$), or double-positive effector cells (DPEC: $CD127^+KLRG1^+$)[52–55]. Several preclinical studies with viral and bacterial infections[56–59] also suggest that EEC, MPEC, and

SLEC populations have similar cytotoxic potential/activity, whereas MPEC and EEC have a higher potential to become long-lived $CD8^+$ T cells[53]. There is also evidence from an *L. monocytogenes*-OVA challenge model in mice that DPEC represent a pool of "intermediate-lived" cells (vs. short-lived SLEC and long-lived MPEC) that rapidly expand into EEC after subsequent infections and contract back into DPEC after infection is resolved[57].

To determine if the diameter of encapsulating biodegradable particle affects CD127/KLRG1 memory subsets of mucosal and systemic $CD8^+$ T cells generated by respiratory immunization with an EP67-conjugated CTL peptide vaccine, we further compared the proportions of CD127/KLRG1 subsets found within $CD8a^+CD44^{Hi}$Tet-$pp89^+$ cells in the lungs and spleen 21 days after respiratory immunization with pp89-RR-EP67 encapsulated in MP or NP (Fig.1B) by flow cytometry (Fig.2). Unencapsulated pp89-RR-EP67 did not increase the proportions of $CD8a^+CD44^{Hi}$Tet-$pp89^+$ cells in the lungs and spleen above vehicle alone (Fig.1A & B, Free vs. PBS) and prevented conclusive comparison of these CD127/KLRG1 subsets.

NP generated ~17% more $CD8a^+CD44^{Hi}$Tet-$pp89^+$ cells with an early effector cell surface phenotype (EEC: $CD127^-KLRG1^-$) than MP (Fig.2A) but ~19% less cells with a memory precursor effector cell surface phenotype (MPEC: $CD127^+KLRG1^-$) (Fig.2B) without affecting proportions of short-lived effector cells (SLEC: $CD127^-KLRG1^+$) [$P = 0.7616$; n=4 mice] (Fig.2C) or double-positive effector cells (DPEC: $CD127^+KLRG1^+$) [$P = 0.7854$; n=4 mice] (Fig.2D). In contrast to the lungs, NP and MP had similar proportions of MPEC (~80% of $CD8a^+CD44^{Hi}$Tet-$pp89^+$ cells), EEC (~18%), SLEC (~2%), and DPEC (~0.1%) in the spleen (not shown). Thus, decreasing the diameter of encapsulating biodegradable particle from ~5.4 μm to ~350 nm changes CD127/KLRG1 subsets of mucosal but not systemic memory $CD8^+$ T cells 21 days after respiratory immunization with an EP67-conjugated CTL peptide vaccine.

The diameter of encapsulating biodegradable particle changes CD127/KRLG1/CD62L memory subsets of systemic $CD8^+$ T cells generated by respiratory immunization with an EP67-conjugated CTL peptide vaccine

Although no differences in CD127/KLRG1 $CD8^+$ T cell subsets were observed between NP and MP in the spleen (not shown), these subsets can further differentiate into effector and central memory subsets based on the expression of the lymph node-homing cell adhesion molecule, CD62L[53, 60]. Upon activation, $CD8^+$ T cells initially down-regulate CD127 and CD62L then re-express CD127. Depending on immunogen availability, $CD8^+$ T cells then differentiate into effector cells (TEFF: $CD127^-KLRG1^-CD62L^-$), effector memory cells (TEM: $CD127^+KLRG1^-CD62L^-$), or re-express CD62L in the absence of immunogen to become central memory cells (TCM: $CD127^+KLRG1^-CD62L^+$)[54]. All three subsets release effector cytokines such as IFN-γ but TEFF cells have the highest cytolytic potential *in vitro* followed by TEM cells[60]. Furthermore, the functional contributions of TCM and TEM against secondary viral challenge are dependent on the nature of the pathogen, route of infection, and model system[58, 59]. Thus, it is likely that the most important T cell subsets for viral protection depend on the host and/or the pathogen[6].

To determine if the diameter of encapsulating biodegradable particle changes CD127/KRLG1/CD62L memory subsets of systemic $CD8^+$ T cells generated by respiratory immunization with an EP67-conjugated CTL peptide vaccine, we further compared CD127/KLRG1/CD62L subsets of $CD8a^+CD44^{Hi}$Tet-$pp89^+$ cells found in the spleen 21 days after respiratory immunization with pp89-RR-EP67 encapsulated in MP or NP (Fig.1C) by flow cytometry (Fig.3). Unencapsulated pp89-RR-EP67 did not increase the proportions of $CD8a^+CD44^{Hi}$Tet-$pp89^+$ cells in the spleen above vehicle alone (Fig.1C, Free vs. PBS) and prevented conclusive comparison of these CD127/KLRG1/CD62L phenotypes. NP generated ~5% more $CD8a^+CD44^{Hi}$Tet-$pp89^+$ cells with a TEFF cell surface phenotype ($CD127^-KLRG1^-CD62L$) (Fig.3A), ~10% more with a TEM cell surface phenotype ($CD127^+KLRG1^-CD62L^-$) (Fig.3B), but ~16% less with a TCM cell surface phenotype ($CD127^+KLRG1^-CD62L^+$) than MP (Fig.3C). Thus, decreasing the diameter of encapsulating biodegradable particle from ~5.4 μm to ~350 nm potentially changes CD127/KLRG1/CD62L memory subsets of systemic $CD8^+$ T cells 21 days after respiratory immunization with an EP67-conjugated CTL peptide vaccine.

The diameter of encapsulating biodegradable particle changes epitope-responsive subsets of mucosal and systemic $CD8^+$ T cells generated by respiratory immunization with an EP67-conjugated CTL peptide vaccine

In addition to memory subsets based on the expression of cell surface markers (i.e., surface phenotype), functional memory subsets of $CD8^+$ T cells can be based on the release of cytokines after exposure to protective epitopes such as pp89 for MCMV (i.e., epitope-responsiveness)[32]. For $CD8^+$ T cells, the secretion of IFN-γ, TNF-α, and/or IL-2 is critical for their effector function *in vivo* and may identify functional subsets of $CD8^+$ T cells that correlate more closely with protection against a given pathogen[32].

To determine if the diameter of encapsulating biodegradable particle changes epitope-responsive subsets of mucosal and systemic $CD8^+$ T cells generated by respiratory immunization with an EP67-conjugated CTL peptide vaccine, we again administered vehicle alone, unencapsulated pp89-RR-EP67, or pp89-RR-EP67 encapsulated in MP (~4.5 μm) or NP (~350 nm) (Table 1) to naïve female BALB/c mice under the same dosage regimen (Fig. 1A) then compared the proportions of pp89-responsive $CD8^+$ cells present in the lungs and spleen 21 days post-immunization by intracellular cytokine staining (ICS) after incubation with pp89 (Fig.4). MP (Fig.4, dark grey bars) and NP (Fig.4, black bars) increased the proportion of pp89-responsive $CD8^+$IFN-γ^+, $CD8^+$TNF-α^+, and $CD8^+$IL-2^+ cells in the lungs (Fig.4A) and $CD8^+$TNF-α^+ cells in the spleen (Fig.4B) to a greater extent than unencapsulated pp89-RR-EP67 (Fig.4, light grey bars) and vehicle alone (Fig.4, PBS). Furthermore, NP increased the proportion of pp89-responsive $CD8^+$IFN-γ^+ cells in the lungs above MP (Fig.4A, black bar vs. dark grey bar), whereas MP increased the proportion of pp89-responsive multifunctional $CD8^+$TNF-α^+IL-2^+ cells in the spleen above NP (Fig. 4B). Thus, decreasing the diameter of encapsulating biodegradable particle from ~5.4 μm to ~350 nm changes epitope-responsive subsets of mucosal and systemic $CD8^+$ T cells generated 21 days after respiratory immunization with an EP67-conjugated CTL peptide vaccine.

Encapsulation in nanoscale biodegradable particles increases the efficacy of respiratory immunization with an EP67-conjugated CTL peptide vaccine

Encapsulation in nanoscale biodegradable particles increases the generation of $CD8^+$ T cell responses after mucosal immunization by increasing uptake by mucosa-associated lymphoid tissue (MALT) and APCs and subsequent cross presentation to MHC I[61]. Furthermore, we found that respiratory immunization with an EP67-based CTL peptide vaccine that included pp89-RR-EP67 increases protection of naïve BALB/c mice against primary respiratory challenge with MCMV and corresponded, in part, with an increase in pp89-specific $CD8^+$ T cells[38]. Thus, encapsulation is expected to increase the efficacy of mucosal immunization with pp89-RR-EP67 against primary respiratory challenge with MCMV and possibly be affected by particle diameter through differences in the total magnitude or CD127/KLRG1/CD62L memory subsets of pp89-specific $CD8^+$ T cells.

To determine if the diameter of the encapsulating biodegradable particle affects protection against primary respiratory infection with MCMV after respiratory immunization with an EP67-conjugated CTL peptide vaccine, we again administered vehicle alone (PBS), unencapsulated pp89-RR-EP67, or pp89-RR-EP67 encapsulated in MP or NP (Table.1) to naïve female BALB/c mice under the same dosage regimen (Fig.1A). We then administered sublethal titers of single mouse-passaged salivary gland-derived MCMV (P1-SGV) intranasally 21 days post-immunization in a volume of PBS expected to deliver P1-SGV to the nasal cavity and lungs (i.e., respiratory challenge) and compared peak titers of productive MCMV in the salivary glands 14 days post-infection by plaque assay (Fig.5A). We focused on protection of the salivary glands because it likely acts as a viral reservoir for the horizontal transmission of CMV[62, 63].

Although NP decreased average peak titers of productive MCMV in the salivary glands to a greater extent below unencapsulated peptide vaccine (~20-fold) [4.8 ± 0.1 (SD) vs. 6.1 ± 0.1 Log_{10} PFU/g salivary glands] (Fig.5B, NP vs. Free) than MP (~10-fold) [5.1 ± 0.2 (SD) vs. 6.1 ± 0.1 Log_{10} PFU/g salivary glands] (Fig.5B, MP vs. Free), there was no statistical difference between encapsulation in MP and NP [5.1 ± 0.2 (SD) vs. 4.8 ± 0.1 Log_{10} PFU/g salivary glands, $P = 0.2105$]. Thus, encapsulating an EP67-conjugated CTL peptide vaccine in biodegradable particles between ~5.4 μm to ~350 nm in diameter increases the efficacy of respiratory immunization against primary respiratory infection with MCMV but is unaffected by particle diameter under the current experimental conditions.

DISCUSSION

Our study provides evidence that decreasing the diameter of the encapsulating biodegradable particle from ~5.4 μm to ~350 nm potentially affects not only the total magnitude but also surface phenotype and epitope-responsive memory subsets of mucosal and systemic $CD8^+$ T cells generated by respiratory immunization with an immunostimulant-conjugated CTL peptide vaccine. We found that 21 days after respiratory immunization of naïve female BALB/c mice with the MCMV CTL peptide vaccine pp89-RR-EP67, decreasing the diameter of encapsulating PLGA 50:50 particles from ~5.4 μm to ~350 nm (i.) increased the magnitude of pp89-specific $CD8^+$ T cells in the lungs and spleen (Fig.1) (ii.) increased pp89-specific early effector cells (EEC: $CD127^-KLRG1^-$) and decreased memory precursor

effector cells (MPEC: $CD127^{+}KLRG1^{-}$) without affecting short-lived effector cells (SLEC: $CD127^{-}KLRG1^{+}$) or double-positive effector cells (DPEC: $CD127^{+}KLRG1^{+}$) in the lungs (Fig.2) or any CD127/KLRG1 memory subsets in the spleen (not shown) (iii.) increased pp89-specific effector cells (TEFF: $CD127^{-}KLRG1^{-}CD62L^{-}$) and effector memory cells (TEM: $CD127^{+}KLRG1^{-}CD62L^{-}$) but decreased central memory cells (TCM: $CD127^{+}KLRG1^{-}CD62L^{+}$) in the spleen (Fig.3) and (iv.) changed subsets of pp89-responsive IFN-γ/TNF-α/IL-2 vaccine-generated $CD8^{+}$ T cells (Fig.4).

Our study also provides evidence that encapsulation in nanoscale biodegradable particles increases the efficacy of primary respiratory immunization with an EP67-conjugated CTL peptide vaccine against primary respiratory infection with MCMV but is unaffected by decreasing the diameter of the encapsulating biodegradable particle from ~5.4 μm to ~350 nm under the current experimental conditions. We found that although primary respiratory immunization against pp89-RR-EP67 encapsulated in ~5.4 μm PLGA 50:50 MP or ~350 nm PLGA 50:50 NP decreased peak titers of productive MCMV in the salivary glands ~10 fold and ~20-fold, respectively, below unencapsulated pp89-RR-EP67 after primary respiratory challenge with P1-SGV, there was no statistical difference between NP and MP (Fig.5B).

There are at least three possible reasons why decreasing the diameter of the encapsulating biodegradable particle from ~5.4 μm to ~350 nm does not increase protection against primary respiratory infection with MCMV. The first possibility is that the difference in the total magnitude of pp89-specific $CD8^{+}$ T cells generated by NP vs. MP was not sufficient to increase protection to detectable levels against productive MCMV in the salivary glands despite observed differences in memory subsets. This is supported by observations that that a higher magnitude of memory T cells can compensate by "mass action"[45] for T cell memory pools that are less responsive to subsequent infections[46]. The second possibility is that the same number of the most protective memory subsets of $CD8^{+}$ T cells against MCMV infection were generated to similar levels by MP and NP despite differences in total magnitude. This is supported by evidence that adoptive transfer of epitope-specific TCM including pp89 are the most effective against primary infection with MCMV[64] and our observation that NP increased the magnitude of pp89-specific $CD8^{+}$ T cells above MP in the spleen (0.81% vs. 0.61%) (Fig.1B) but had the same levels of total TCM ($CD127^{+}KLRG1^{-}CD62L^{+}$) (~0.38% of total $CD8a^{+}CD44^{HI}$Tet-pp89^{+} cells; NP: ~45.9% of 0.81% and MP: ~62% of 0.61%) (Fig.3C). The third possibility is that differences in protection by CD127/KLRG1/CD62L memory subsets becomes more apparent at later time points when potentially short-lived memory subsets are no longer around to provide protection. This is supported by evidence that adoptive transfer of a mixture of epitope-specific TEM ($CD8^{+}CD44^{HI}CD127^{HI}CD62^{LO}$) and TCM ($CD8^{+}CD44^{HI}CD127^{HI}CD62L^{HI}$) stably protects C576BL/6 mice against multiple challenges with MCMV over the course of 180 days more effectively than TEFF ($CD8^{+}CD44^{HI}CD127^{LO}$)[65] and our own observation that NP and MP generated different proportions of TEFF and TEM/TCM (Fig.3).

Ideal diameter for encapsulation in nanoscale biodegradable particles?

Similar to our studies, decreasing the diameter of PLGA 50:50 particles co-encapsulating CpG or Poly (I:C) and ovalbumin from ~17 μm to ~300 nm (CpG)[30] or from ~110 μm to ~350 nm (Poly (I:C))[31] increases the magnitude of memory $CD8^+$ T cells in mice after systemic (SQ) immunization. Furthermore, decreasing the diameter of poly(sebacic anhydride) [poly(SA)] particles from ~2.5 μm to ~470 nm or ~360 nm increases the rate of deposition in the respiratory tract of mice after IN administration in 50 μL PBS[66]. This suggests that encapsulation in biodegradable particles within the ~300 nm diameter range is ideal for maximizing the magnitude of the memory $CD8^+$ and possibly $CD4^+$ T cell pool generated by systemic or mucosal immunization. It is likely, however, that the magnitude of the memory pool will continue to increase at diameters below 300 nm to some lower limit because decreasing the diameter of polypropylene sulfide particles from 200 nm to 30 nm decreases the magnitude of epitope-specific $CD4^+$ T cells in the lungs against conjugated OVA after IN administration[67].

In contrast to $CD8^+$ T cells, decreasing the diameter of encapsulating biodegradable particle from 8 μm to < 2 μm[68] decreases the generation of serum IgG after systemic immunization and decreasing the diameter from 4 μm to 600 nm[69], 14 μm to 4 μm[70] or 1 μm to 200 nm[71] decreases the generation of serum IgG against encapsulated protein after oral[69] or intranasal immunization[70, 71], respectively. This suggests that the ideal encapsulating diameter for antibodies is in the micrometer range. Furthermore, it remains to be determined whether similar trends in particle diameters occur in larger animal models or humans and will require tight control over the distribution of particle diameters as well as the use of the most effective diameter characterization techniques[29]. There is also evidence that the surface chemistry of the particle can affect the rate of uptake by human dendritic cells *in vitro*[72]. As such, identifying the optimal diameter for this dosage form will ultimately depend on how it affects the required protective immune response(s) against a specific pathogen in a given host, tight control and characterization of particle diameter, and possible confounding effects by the surface chemistry and composition of the encapsulating particle.

Possible role of the diameter of encapsulating biodegradable particle in the magnitude and memory subsets of $CD8^+$ T cells generated by respiratory immunization with an EP67-conjugated CTL peptide vaccine—In a murine model that closely resembles immunization with subunit vaccines, the process of T cell expansion and memory formation consists of three phases that begin when naïve T cells enter lymph nodes (LN) containing activated DCs that have a high level of epitope presentation in MHCI (pMHCI)[73]. Phase 1 (up to ~8 hrs long) involves transient interactions between T cells and activated Ag-pulsed DCs until a sufficient level of antigenic stimuli from each T cell-DC encounter triggers a transition to Phase 2. Phase 2 involves longer lasting T cell-DC interactions (at least 30 min), the formation of mature immunological synapses between T cells and individual activated DC-pMHCI, and the upregulation of T cell activation markers and cytokines (~12 hrs long). Phase 3 begins within 24 hrs of naïve T cells entering the LN and again involves transient interactions between T cells and DCs but with vigorous T cell proliferation.

The transition from Phase 1 to Phase 2 is required for eventual sustained T cell expansion and the development of long-lived memory T cells[74]. At very low pMHCI surface densities on activated DCs, T cells rapidly expand but don't progress to Phase 2 and eventually rapidly contract within 96 hrs, whereas increasing the number of LPS-activated DCs per LN and surface density of pMHCI per activated DC increases the rate of transition from Phase 1 to Phase 2[75]. Thus, although not directly investigated, intermediate numbers of activated DCs per LN and pMHCI surface densities per activated DC likely have effects on the magnitude of the T cell pool and, possibly, the proportions of memory subsets. The process of memory T cell development is also affected by the cytokine microenvironment and presence of Th cells and neutrophils in secondary lymphoid organs[59, 76]. As such, it is possible that encapsulation in NP or MP ultimately affects the total magnitude and memory subsets of mucosal and systemic $CD8^+$ T cells generated by mucosal immunization through different effects on the magnitude and kinetics of activated DC-pMHCI / surface densities of pMHCI as well as the cytokine microenvironment in MALT-draining LN and the spleen.

With the above model in mind, NP may increase the total magnitude of the mucosal and systemic $CD8^+$ T cell memory pool (Day 21 post-immunization for this study) over MP, in part, by first increasing the rate that encapsulated pp89-RR-EP67 localizes to the MALT and spleen. This is supported by observations that (i.) decreasing the diameter of poly(SA) particles from 2.5 μM to 360 nm increases deposition in the respiratory tract of mice within at least 6 hrs after IN administration in 50 μL PBS[66] (ii.) decreasing the diameter of polystyrene particles from 2 μm to 200 nm increases the rate of NALT uptake in human adenoid tissues[77] and (iii.) both 7 μm styrene-divinyl benzene microspheres[20] and 1.1 μm polystyrene microspheres[19] translocate to the spleen after IN administration in 50 μL PBS at a rate that is likely dependent on particle diameter.

After arriving in the MALT, NP may be internalized at a faster rate than MP by migrating DCs and cross-present CTL epitopes in MHCI to a greater extent and for a longer duration. A similar effect may occur with NP localizing to the spleen but through direct interactions with resident DCs. This increase in the amount of NP delivered to the draining-LN and spleen and the rate of DC internalization then increases and sustains a greater number of activated DC with higher surface densities of pMHCI in MALT-draining LN and the spleen, leading to an increase in the rate of transition from Phase 1 to Phase 2 during T cell expansion and subsequent number of T cells that transition to the $CD8^+$ T cell memory pool. This model is supported, in part, by observations that (i.) decreasing the diameter of PLGA 50:50 particles co-encapsulating CpG and OVA from 7 μm to 300 nm or PLGA 50:50 particles containing co-encapsulated poly(I:C) and OVA from ~17 μm to ~357 nm increases the rate of internalization in a human DC cell line[30] or an immature murine dendritic cell line[31], respectively (ii.) decreasing the diameter of PLGA 50:50 particles containing co-encapsulated poly(I:C) and OVA from ~17 μm to ~357 nm increases MHCI presentation[31] (iii.) encapsulation of OVA in PLGA between ~500 nm and 1 μm increases the duration of MHCI presentation in mouse bone marrow-derived dendritic cells (BMDCs) *in vitro* compared to soluble OVA[17] and (iv.) decreasing the diameter of polystyrene particles from 1 μm to 20 nm increases the rate of uptake by lung parenchyma DC and migrating DC in lung draining-LN of mice within 24 hrs of IN administration[78]. Differential internalization by subsets of DCs and macrophages is also an additional consideration although co-

encapsulation of CpG and OVA in PLGA 50:50 microspheres increases cross-presentation in both cell types *in vitro* and *in vivo*[79]. Possible differences in the generation of long-term T cell memory responses by either cell type alone *in vivo*, however, was not determined.

Again, with the above model in mind, differences in the memory subsets between NP and MP, could also be due to differences in effects on the 3-phase model of T cell expansion and the subsequent kinetics of memory development by differences in the rates of particle localization to the MALT, draining LN, and the spleen. As such, the proportions of memory subsets at 21 days post-immunization may reflect differences in the kinetics of memory development and eventually become similar at later time points.

Given that pp89-RR-EP67 alone is active after respiratory immunization[38] but unlikely to directly stimulate neutrophils in the draining LN[35] and the possibility that 2 to 8 μm particles are not phagocytosed by APCs *in vivo*[80], the contributions of released vs. encapsulated peptide vaccine during particle localization to the MALT-draining LN and the spleen by our 5 μm diameter MP can also not be overlooked. There is also the possibility that NP and MP have different effects on the cytokine microenvironment in MALT-draining LN and the spleen through different direct effects on macrophages and DCs[81].

CONCLUSIONS

In summary, our findings indicate that the diameter of encapsulating nanoscale biodegradable particles potentially affects the total magnitude, effector/central memory subsets, and epitope-responsive subsets of mucosal and systemic epitope-specific $CD8^+$ T cells generated by respiratory immunization with an encapsulated EP67-conjugated CTL peptide vaccine. Thus, varying the diameter of nanoscale biodegradable particles containing co-encapsulated immunostimulants (conjugated or free) and subunit vaccines may increase the efficacy of mucosal vaccines against certain pathogens by selectively increasing the magnitude of one or more $CD8^+$ T cell memory subsets that correlate the strongest with clinically defined protection.

Supplementary Material

Refer to Web version on PubMed Central for supplementary material.

Acknowledgments

This work was supported by NIH COBRE 2P20GM103480/NCRR (Nebraska Center for Nanomedicine) (JAV), NIH R01AI121050/NIAID (JAV), NIH R41AI094710/NIAID (SDS), the UNMC Edna Ittner Research Fund (JAV), and UNMC Predoctoral Fellowships (VKK, SBT). We thank Victoria Smith M.S. and Dr. Philip Hexley for assistance with the FACS studies and the NIH Tetramer Core Facility (Contract HHSN272201300006C) for providing (MHC) tetramers. The UNMC Flow Cytometry Research Facility is managed through the Office of the Vice Chancellor for Research and supported by state funds from the Nebraska Research Initiative (NRI) and The Fred and Pamela Buffet Cancer Center's National Cancer Institute Cancer Support Grant.

References

1. Plotkin SA. Complex correlates of protection after vaccination. Clinical infectious diseases : an official publication of the Infectious Diseases Society of America. 2013; 56(10):1458–65. [PubMed: 23386629]

2. Nguipdop Djomo, P., Thomas, SL., Fine, PEM. Innitiative for Vaccine Research (IVR) of the Department of Immunization. Vaccines and Biologicals: World Health Organization; 2013. Correlates of vaccine-induced protection: methods and implications; p. 1-49.
3. Thakur A, Pedersen LE, Jungersen G. Immune markers and correlates of protection for vaccine induced immune responses. Vaccine. 2012; 30(33):4907–20. [PubMed: 22658928]
4. Rappuoli R. Bridging the knowledge gaps in vaccine design. Nat Biotechnol. 2007; 25(12):1361–6. [PubMed: 18066025]
5. Griffiths KL, Khader SA. Novel vaccine approaches for protection against intracellular pathogens. Current opinion in immunology. 2014; 28:58–63. [PubMed: 24608070]
6. Amanna IJ, Slifka MK. Contributions of humoral and cellular immunity to vaccine-induced protection in humans. Virology. 2011; 411(2):206–15. [PubMed: 21216425]
7. Igietseme JU, Eko FO, He Q, Black CM. Antibody regulation of Tcell immunity: implications for vaccine strategies against intracellular pathogens. Expert Rev Vaccines. 2004; 3(1):23–34. [PubMed: 14761241]
8. Lycke N. Recent progress in mucosal vaccine development: potential and limitations. Nature reviews. Immunology. 2012; 12(8):592–605.
9. Kraehenbuhl JP, Neutra MR. Mucosal vaccines: where do we stand? Curr Top Med Chem. 2013; 13(20):2609–28. [PubMed: 24066889]
10. Levine MM. Immunogenicity and efficacy of oral vaccines in developing countries: lessons from a live cholera vaccine. BMC biology. 2010; 8:129. [PubMed: 20920375]
11. Purcell AW, McCluskey J, Rossjohn J. More than one reason to rethink the use of peptides in vaccine design. Nat Rev Drug Discov. 2007; 6(5):404–14. [PubMed: 17473845]
12. Moyle PM, Toth I. Modern subunit vaccines: development, components, and research opportunities. ChemMedChem. 2013; 8(3):360–76. [PubMed: 23316023]
13. Schlosser E, Mueller M, Fischer S, Basta S, Busch DH, Gander B, Groettrup M. TLR ligands and antigen need to be coencapsulated into the same biodegradable microsphere for the generation of potent cytotoxic T lymphocyte responses. Vaccine. 2008; 26(13):1626–37. [PubMed: 18295941]
14. Joshi VB, Geary SM, Salem AK. Biodegradable particles as vaccine antigen delivery systems for stimulating cellular immune responses. Hum Vaccin Immunother. 2013; 9(12):2584–90. [PubMed: 23978910]
15. Eldridge JH, Meulbroek JA, Staas JK, Tice TR, Gilley RM. Vaccine-containing biodegradable microspheres specifically enter the gut-associated lymphoid tissue following oral administration and induce a disseminated mucosal immune response. Advances in experimental medicine and biology. 1989; 251:191–202. [PubMed: 2610110]
16. Demento SL, Cui W, Criscione JM, Stern E, Tulipan J, Kaech SM, Fahmy TM. Role of sustained antigen release from nanoparticle vaccines in shaping the T cell memory phenotype. Biomaterials. 2012; 33(19):4957–64. [PubMed: 22484047]
17. Shen H, Ackerman AL, Cody V, Giodini A, Hinson ER, Cresswell P, Edelson RL, Saltzman WM, Hanlon DJ. Enhanced and prolonged cross-presentation following endosomal escape of exogenous antigens encapsulated in biodegradable nanoparticles. Immunology. 2006; 117(1):78–88. [PubMed: 16423043]
18. Audran R, Peter K, Dannull J, Men Y, Scandella E, Groettrup M, Gander B, Corradin G. Encapsulation of peptides in biodegradable microspheres prolongs their MHC class-I presentation by dendritic cells and macrophages in vitro. Vaccine. 2003; 21(11–12):1250–5. [PubMed: 12559806]
19. Eyles JE, Bramwell VW, Williamson ED, Alpar HO. Microsphere translocation and immunopotentiation in systemic tissues following intranasal administration. Vaccine. 2001; 19(32):4732–42. [PubMed: 11535324]
20. Eyles JE, Spiers ID, Williamson ED, Alpar HO. Tissue distribution of radioactivity following intranasal administration of radioactive microspheres. J Pharm Pharmacol. 2001; 53(5):601–7. [PubMed: 11370699]
21. Fischer S, Schlosser E, Mueller M, Csaba N, Merkle HP, Groettrup M, Gander B. Concomitant delivery of a CTL-restricted peptide antigen and CpG ODN by PLGA microparticles induces cellular immune response. Journal of drug targeting. 2009; 17(8):652–61. [PubMed: 19622019]

22. Silva AL, Rosalia RA, Sazak A, Carstens MG, Ossendorp F, Oostendorp J, Jiskoot W. Optimization of encapsulation of a synthetic long peptide in PLGA nanoparticles: low-burst release is crucial for efficient CD8(+) T cell activation. European journal of pharmaceutics and biopharmaceutics : official journal of Arbeitsgemeinschaft fur Pharmazeutische Verfahrenstechnik e.V. 2013; 83(3):338–45. [PubMed: 23201055]
23. Ma W, Chen M, Kaushal S, McElroy M, Zhang Y, Ozkan C, Bouvet M, Kruse C, Grotjahn D, Ichim T, Minev B. PLGA nanoparticle-mediated delivery of tumor antigenic peptides elicits effective immune responses. Int J Nanomedicine. 2012; 7:1475–87. [PubMed: 22619507]
24. Mohan T, Sharma C, Bhat AA, Rao DN. Modulation of HIV peptide antigen specific cellular immune response by synthetic alpha- and beta-defensin peptides. Vaccine. 2013; 31(13):1707–16. [PubMed: 23384751]
25. Zhang Z, Tongchusak S, Mizukami Y, Kang YJ, Ioji T, Touma M, Reinhold B, Keskin DB, Reinherz EL, Sasada T. Induction of anti-tumor cytotoxic T cell responses through PLGA-nanoparticle mediated antigen delivery. Biomaterials. 2011; 32(14):3666–78. [PubMed: 21345488]
26. Xiang SD, Scholzen A, Minigo G, David C, Apostolopoulos V, Mottram PL, Plebanski M. Pathogen recognition and development of particulate vaccines: does size matter? Methods. 2006; 40(1):1–9. [PubMed: 16997708]
27. Oyewumi MO, Kumar A, Cui Z. Nano-microparticles as immune adjuvants: correlating particle sizes and the resultant immune responses. Expert Rev Vaccines. 2010; 9(9):1095–107. [PubMed: 20822351]
28. Silva AL, Soema PC, Slutter B, Ossendorp F, Jiskoot W. PLGA particulate delivery systems for subunit vaccines: Linking particle properties to immunogenicity. Hum Vaccin Immunother. 2016; 12(4):1056–69. [PubMed: 26752261]
29. Slutter B, Jiskoot W. Sizing the optimal dimensions of a vaccine delivery system: a particulate matter. Expert Opin Drug Deliv. 2016; 13(2):167–70. [PubMed: 26578092]
30. Joshi VB, Geary SM, Salem AK. Biodegradable particles as vaccine delivery systems: size matters. AAPS J. 2013; 15(1):85–94. [PubMed: 23054976]
31. Silva AL, Rosalia RA, Varypataki E, Sibuea S, Ossendorp F, Jiskoot W. Poly-(lactic-co-glycolic-acid)-based particulate vaccines: particle uptake by dendritic cells is a key parameter for immune activation. Vaccine. 2015; 33(7):847–54. [PubMed: 25576216]
32. Seder RA, Darrah PA, Roederer M. T-cell quality in memory and protection: implications for vaccine design. Nature reviews. Immunology. 2008; 8(4):247–58.
33. Bolton DL, Roederer M. Flow cytometry and the future of vaccine development. Expert Rev Vaccines. 2009; 8(6):779–89. [PubMed: 19485757]
34. Busch DH, Frassle SP, Sommermeyer D, Buchholz VR, Riddell SR. Role of memory T cell subsets for adoptive immunotherapy. Semin Immunol. 2016; 28(1):28–34. [PubMed: 26976826]
35. Vogen SM, Paczkowski NJ, Kirnarsky L, Short A, Whitmore JB, Sherman SA, Taylor SM, Sanderson SD. Differential activities of decapeptide agonists of human C5a: the conformational effects of backbone N-methylation. Int Immunopharmacol. 2001; 1(12):2151–62. [PubMed: 11710544]
36. Taylor SM, Sherman SA, Kirnarsky L, Sanderson SD. Development of response-selective agonists of human C5a anaphylatoxin: conformational, biological, and therapeutic considerations. Curr Med Chem. 2001; 8(6):675–84. [PubMed: 11281848]
37. Morgan EL, Morgan BN, Stein EA, Vitrs EL, Thoman ML, Sanderson SD, Phillips JA. Enhancement of in vivo and in vitro immune functions by a conformationally biased, response-selective agonist of human C5a: implications for a novel adjuvant in vaccine design. Vaccine. 2009; 28(2):463–9. [PubMed: 19836478]
38. Karuturi BV, Tallapaka SB, Phillips JA, Sanderson SD, Vetro JA. Preliminary evidence that the novel host-derived immunostimulant EP67 can act as a mucosal adjuvant. Clinical immunology. 2015; 161(2):251–9. [PubMed: 26111481]
39. Reddehase MJ, Rothbard JB, Koszinowski UH. A pentapeptide as minimal antigenic determinant for MHC class I-restricted T lymphocytes. Nature. 1989; 337(6208):651–3. [PubMed: 2465495]

40. Ulrich JT, Cieplak W, Paczkowski NJ, Taylor SM, Sanderson SD. Induction of an antigen-specific CTL response by a conformationally biased agonist of human C5a anaphylatoxin as a molecular adjuvant. Journal of immunology. 2000; 164(10):5492–8.
41. Sah H. A new strategy to determine the actual protein content of poly(lactide-co-glycolide) microspheres. Journal of pharmaceutical sciences. 1997; 86(11):1315–8. [PubMed: 9383747]
42. Karuturi VK, Tallapaka SB, Phillips JA, Sanderson SD, Vetro JA. Preliminary evidence that the novel host-derived immunostimulant EP67 can act as a mucosal adjuvant. Clinical immunology. 2015
43. Southam DS, Dolovich M, O'Byrne PM, Inman MD. Distribution of intranasal instillations in mice: effects of volume, time, body position, and anesthesia. American journal of physiology. Lung cellular and molecular physiology. 2002; 282(4):L833–9. [PubMed: 11880310]
44. Ye M, Morello CS, Spector DH. Strong CD8 T-cell responses following coimmunization with plasmids expressing the dominant pp89 and subdominant M84 antigens of murine cytomegalovirus correlate with long-term protection against subsequent viral challenge. Journal of virology. 2002; 76(5):2100–12. [PubMed: 11836387]
45. Ganusov VV, Barber DL, De Boer RJ. Killing of targets by CD8 T cells in the mouse spleen follows the law of mass action. PloS one. 2011; 6(1):e15959. [PubMed: 21283669]
46. Messingham KA, Badovinac VP, Harty JT. Deficient anti-listerial immunity in the absence of perforin can be restored by increasing memory CD8+ T cell numbers. Journal of immunology. 2003; 171(8):4254–62.
47. Bunde T, Kirchner A, Hoffmeister B, Habedank D, Hetzer R, Cherepnev G, Proesch S, Reinke P, Volk HD, Lehmkuhl H, Kern F. Protection from cytomegalovirus after transplantation is correlated with immediate early 1-specific CD8 T cells. J Exp Med. 2005; 201(7):1031–6. [PubMed: 15795239]
48. Whitton JL, Slifka MK, Liu F, Nussbaum AK, Whitmire JK. The regulation and maturation of antiviral immune responses. Adv Virus Res. 2004; 63:181–238. [PubMed: 15530562]
49. Haluszczak C, Akue AD, Hamilton SE, Johnson LD, Pujanauski L, Teodorovic L, Jameson SC, Kedl RM. The antigen-specific CD8+ T cell repertoire in unimmunized mice includes memory phenotype cells bearing markers of homeostatic expansion. J Exp Med. 2009; 206(2):435–48. [PubMed: 19188498]
50. Schluns KS, Kieper WC, Jameson SC, Lefrancois L. Interleukin-7 mediates the homeostasis of naive and memory CD8 T cells in vivo. Nature immunology. 2000; 1(5):426–32. [PubMed: 11062503]
51. Kaech SM, Tan JT, Wherry EJ, Konieczny BT, Surh CD, Ahmed R. Selective expression of the interleukin 7 receptor identifies effector CD8 T cells that give rise to long-lived memory cells. Nature immunology. 2003; 4(12):1191–8. [PubMed: 14625547]
52. Ahlers JD, Belyakov IM. Memories that last forever: strategies for optimizing vaccine T-cell memory. Blood. 2010; 115(9):1678–89. [PubMed: 19903895]
53. Obar JJ, Lefrancois L. Memory CD8+ T cell differentiation. Annals of the New York Academy of Sciences. 2010; 1183:251–66. [PubMed: 20146720]
54. Obar JJ, Lefrancois L. Early signals during CD8 T cell priming regulate the generation of central memory cells. Journal of immunology. 2010; 185(1):263–72.
55. Obar JJ, Lefrancois L. Early events governing memory CD8+ T-cell differentiation. International immunology. 2010; 22(8):619–25. [PubMed: 20504887]
56. Kaech SM, Cui W. Transcriptional control of effector and memory CD8+ T cell differentiation. Nature reviews. Immunology. 2012; 12(11):749–61.
57. Obar JJ, Jellison ER, Sheridan BS, Blair DA, Pham QM, Zickovich JM, Lefrancois L. Pathogen-induced inflammatory environment controls effector and memory CD8+ T cell differentiation. Journal of immunology. 2011; 187(10):4967–78.
58. Roberts AD, Woodland DL. Cutting edge: effector memory CD8+ T cells play a prominent role in recall responses to secondary viral infection in the lung. Journal of immunology. 2004; 172(11): 6533–7.
59. Sallusto F, Geginat J, Lanzavecchia A. Central memory and effector memory T cell subsets: function, generation, and maintenance. Annual review of immunology. 2004; 22:745–63.

60. Lefrancois L, Obar JJ. Once a killer, always a killer: from cytotoxic T cell to memory cell. Immunological reviews. 2010; 235(1):206–18. [PubMed: 20536565]

61. Woodrow KA, Bennett KM, Lo DD. Mucosal vaccine design and delivery. Annual review of biomedical engineering. 2012; 14:17–46.

62. Crough T, Khanna R. Immunobiology of human cytomegalovirus: from bench to bedside. Clinical microbiology reviews. 2009; 22(1):76–98. Table of Contents. [PubMed: 19136435]

63. Boeckh M, Geballe AP. Cytomegalovirus: pathogen, paradigm, and puzzle. J Clin Invest. 2011; 121(5):1673–80. [PubMed: 21659716]

64. Ebert S, Podlech J, Gillert-Marien D, Gergely KM, Buttner JK, Fink A, Freitag K, Thomas D, Reddehase MJ, Holtappels R. Parameters determining the efficacy of adoptive CD8 T-cell therapy of cytomegalovirus infection. Med Microbiol Immunol. 2012; 201(4):527–39. [PubMed: 22972232]

65. Quinn M, Turula H, Tandon M, Deslouches B, Moghbeli T, Snyder CM. Memory T cells specific for murine cytomegalovirus re-emerge after multiple challenges and recapitulate immunity in various adoptive transfer scenarios. Journal of immunology. 2015; 194(4):1726–36.

66. Brenza TM, Petersen LK, Zhang Y, Huntimer LM, Ramer-Tait AE, Hostetter JM, Wannemuehler MJ, Narasimhan B. Pulmonary biodistribution and cellular uptake of intranasally administered monodisperse particles. Pharmaceutical research. 2015; 32(4):1368–82. [PubMed: 25297714]

67. Stano A, Nembrini C, Swartz MA, Hubbell JA, Simeoni E. Nanoparticle size influences the magnitude and quality of mucosal immune responses after intranasal immunization. Vaccine. 2012; 30(52):7541–6. [PubMed: 23103199]

68. Katare YK, Muthukumaran T, Panda AK. Influence of particle size, antigen load, dose and additional adjuvant on the immune response from antigen loaded PLA microparticles. Int J Pharm. 2005; 301(1–2):149–60. [PubMed: 16023313]

69. Tabata Y, Inoue Y, Ikada Y. Size effect on systemic and mucosal immune responses induced by oral administration of biodegradable microspheres. Vaccine. 1996; 14(17–18):1677–85. [PubMed: 9032899]

70. Uchida T, Goto S. Oral delivery of poly(lactide-co-glycolide) microspheres containing ovalbumin as vaccine formulation: particle size study. Biol Pharm Bull. 1994; 17(9):1272–6. [PubMed: 7841952]

71. Gutierro I, Hernandez RM, Igartua M, Gascon AR, Pedraz JL. Size dependent immune response after subcutaneous, oral and intranasal administration of BSA loaded nanospheres. Vaccine. 2002; 21(1–2):67–77. [PubMed: 12443664]

72. Foged C, Brodin B, Frokjaer S, Sundblad A. Particle size and surface charge affect particle uptake by human dendritic cells in an in vitro model. Int J Pharm. 2005; 298(2):315–22. [PubMed: 15961266]

73. Mempel TR, Henrickson SE, Von Andrian UH. T-cell priming by dendritic cells in lymph nodes occurs in three distinct phases. Nature. 2004; 427(6970):154–9. [PubMed: 14712275]

74. Henrickson SE, Perro M, Loughhead SM, Senman B, Stutte S, Quigley M, Alexe G, Iannacone M, Flynn MP, Omid S, Jesneck JL, Imam S, Mempel TR, Mazo IB, Haining WN, von Andrian UH. Antigen availability determines CD8(+) T cell-dendritic cell interaction kinetics and memory fate decisions. Immunity. 2013; 39(3):496–507. [PubMed: 24054328]

75. Henrickson SE, Mempel TR, Mazo IB, Liu B, Artyomov MN, Zheng H, Peixoto A, Flynn MP, Senman B, Junt T, Wong HC, Chakraborty AK, von Andrian UH. T cell sensing of antigen dose governs interactive behavior with dendritic cells and sets a threshold for T cell activation. Nature immunology. 2008; 9(3):282–91. [PubMed: 18204450]

76. Leliefeld PHC, Koenderman L, Pillay J. How Neutrophils Shape Adaptive Immune Responses. Frontiers in immunology. 2015; 6:471. [PubMed: 26441976]

77. Fujimura Y, Akisada T, Harada T, Haruma K. Uptake of microparticles into the epithelium of human nasopharyngeal lymphoid tissue. Med Mol Morphol. 2006; 39(4):181–6. [PubMed: 17187179]

78. Blank F, Stumbles PA, Seydoux E, Holt PG, Fink A, Rothen-Rutishauser B, Strickland DH, von Garnier C. Size-dependent uptake of particles by pulmonary antigen-presenting cell populations

and trafficking to regional lymph nodes. American journal of respiratory cell and molecular biology. 2013; 49(1):67–77. [PubMed: 23492193]

79. Schliehe C, Redaelli C, Engelhardt S, Fehlings M, Mueller M, van Rooijen N, Thiry M, Hildner K, Weller H, Groettrup M. CD8- dendritic cells and macrophages cross-present poly(D,L-lactate-co-glycolate) acid microsphere-encapsulated antigen in vivo. Journal of immunology. 2011; 187(5): 2112–21.
80. Kanchan V, Panda AK. Interactions of antigen-loaded polylactide particles with macrophages and their correlation with the immune response. Biomaterials. 2007; 28(35):5344–57. [PubMed: 17825905]
81. Yue H, Wei W, Yue Z, Lv P, Wang L, Ma G, Su Z. Particle size affects the cellular response in macrophages. Eur J Pharm Sci. 2010; 41(5):650–7. [PubMed: 20870022]

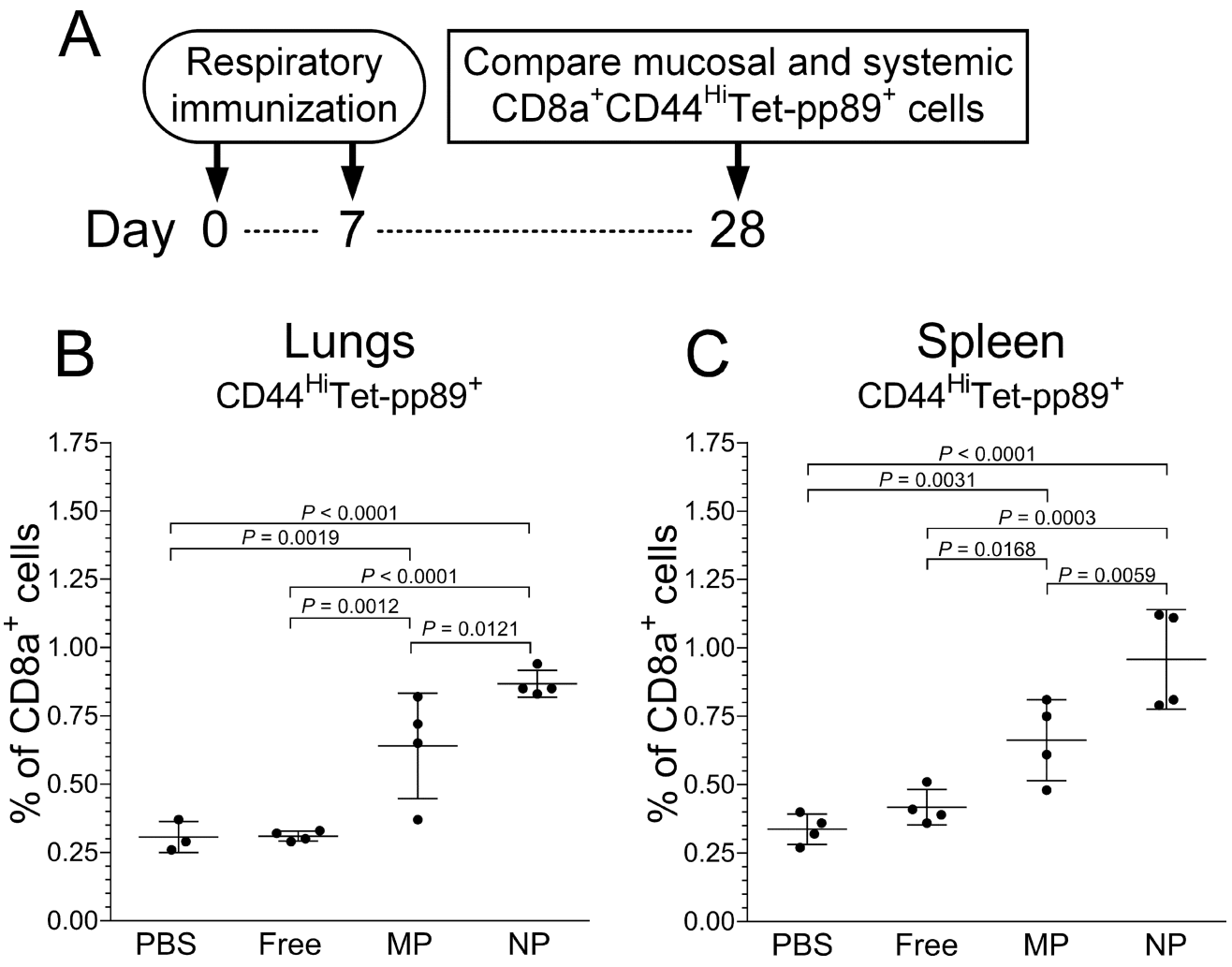

Figure 1.

The diameter of encapsulating biodegradable particle affects the proportion of mucosal and systemic epitope-specific $CD8^+$ T cells generated by respiratory immunization with an EP67-conjugated CTL peptide vaccine. A protective MCMV CTL epitope in BALB/c mice, pp89, was individually conjugated to the N-terminal of EP67 through a lysosomal protease-labile double arginine (RR) linker (pp89-RR-EP67). (A) Vehicle alone (PBS), unencapsulated pp89-RR-EP67 (Free, 50 μg), or the same dose of pp89-RR-EP67 encapsulated in ~5.4 μm PLGA 50:50 microparticles (MP) or ~350 nm PLGA 50:50 nanoparticles (NP) was then administered to naïve female BALB/c mice (~4 wk old) (50 μL IN) on Day 0 and Day 7. Twenty-one days after immunization (Day 28), the average percent of $CD8a^+CD44^{Hi}$ cells that were Tet-$pp89^+$ ± SD (n=4 mice) in the (B) lungs and (C) spleen was determined by flow cytometry then compared by ordinary one-way ANOVA with uncorrected Fisher's LSD test. Data are representative of at least two independent experiments.

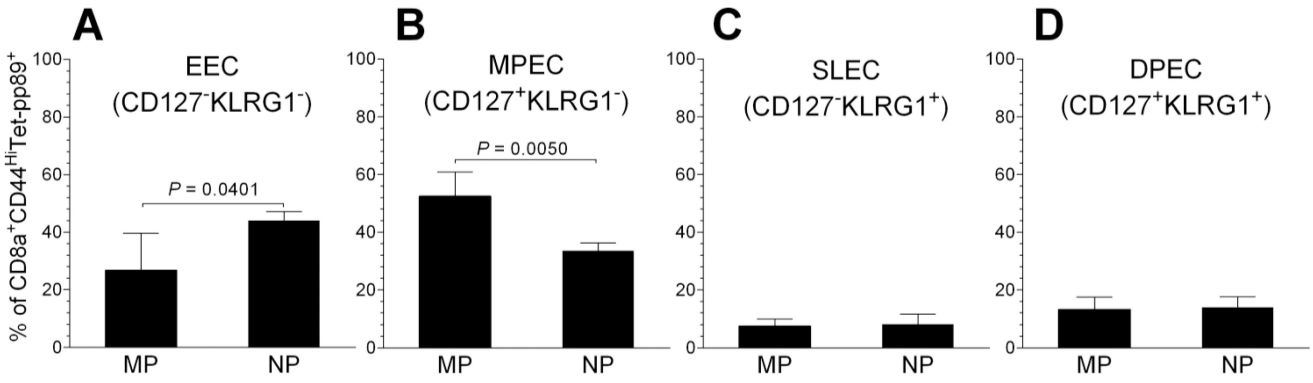

Figure 2.

The diameter of encapsulating biodegradable particle affects CD127/KLRG1 memory subsets of mucosal $CD8^+$ T cells generated by respiratory immunization with an EP67-conjugated CTL peptide vaccine. Twenty-one days after respiratory immunization of naïve female BALB/c mice (~4 wk old) with pp89-RR-EP67 encapsulated in ~5.4 μm PLGA 50:50 microparticles (MP) or ~350 nm PLGA 50:50 nanoparticles (NP) (Fig.1), the average percent of $CD8a^+CD44^{Hi}$Tet-$pp89^+$ cells ± SD (n=4 mice) in the lungs that were (A) early effector cells (EEC: CD127KLRG1), (B) memory precursor effector cells (MPEC: $CD127^+$KLRG1), (C) short-lived effector cells (SLEC: CD127$KLRG1^+$), or (D) double-positive effector cells (DPEC: $CD127^+KLRG1^+$) was determined by flow cytometry and compared by two-tailed unpaired *t*-test. Unencapsulated pp89-RR-EP67 generated similar proportions of $CD8a^+CD44^{Hi}$Tet-$pp89^+$ cells in the lungs as PBS vehicle alone (Fig.1A, Free vs. PBS) and prevented conclusive comparison of these CD127/KLRG1 phenotypes. No differences in CD127/KLRG1 subsets were observed in the spleen (not shown). Data are representative of at least two independent experiments.

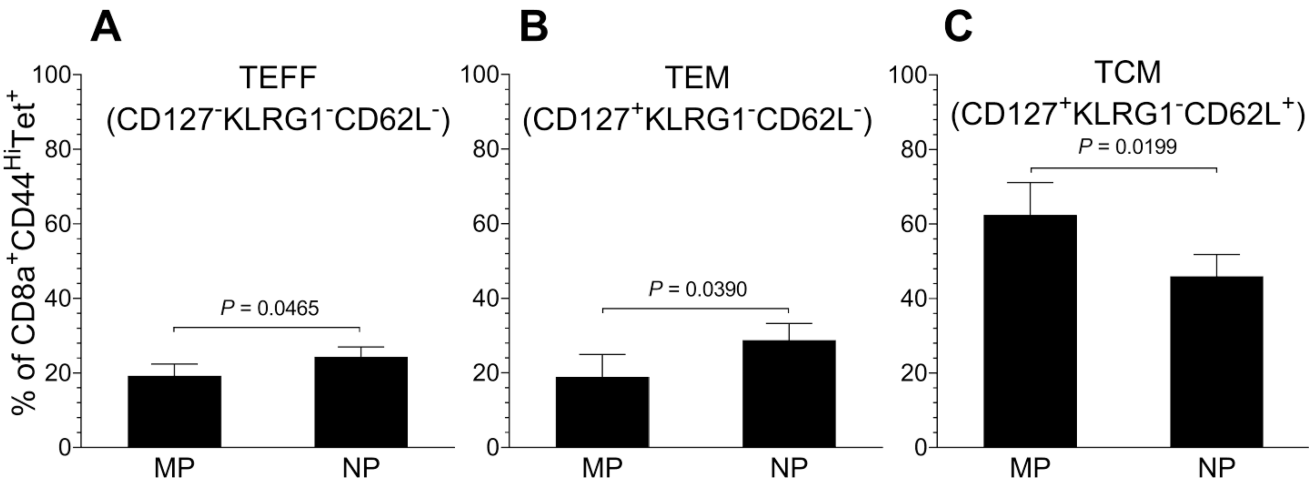

Figure 3.

The diameter of encapsulating biodegradable particle affects CD127/KRLG1/CD62L memory subsets of systemic $CD8^+$ T cells generated by respiratory immunization with an EP67-conjugated CTL peptide vaccine. Twenty-one days after respiratory immunization of naïve female BALB/c mice (~4 wk old) with pp89-RR-EP67 encapsulated in ~5.4 μm PLGA 50:50 microparticles (MP) or ~350 nm PLGA 50:50 nanoparticles (NP) (Fig.1), the average percent of $CD8a^+CD44^{Hi}$Tet-$pp89^+$ cells ± SD (n=4 mice) in the spleen that were (A) effector cells (TEFF: CD127KLRG1CD62L), (B) effector memory cells (TEM: $CD127^+$KLRG1CD62L), or (C) central memory cells (TCM: $CD127^+$KLRG1$CD62L^+$) was determined by flow cytometry and compared by two-tailed unpaired *t*-test. Unencapsulated pp89-RR-EP67 generated similar proportions of $CD8a^+CD44^{Hi}$Tet-$pp89^+$ cells in the spleen as PBS vehicle alone (Fig.1B, Free vs. PBS) and prevented conclusive comparison of these CD127/KRLG1/CD62L phenotypes. Data are representative of at least two independent experiments.

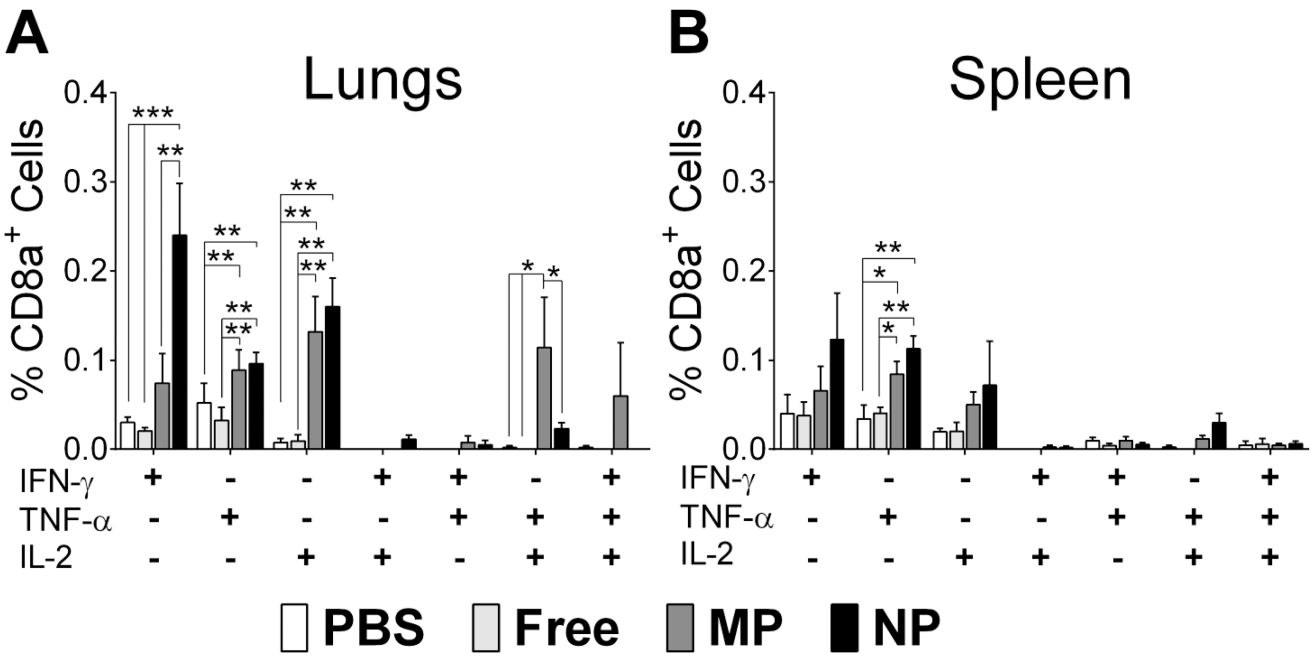

Figure 4.

The diameter of encapsulating biodegradable particle affects epitope-responsive subsets of mucosal and systemic $CD8^+$ T cells generated by respiratory immunization with an EP67-conjugated CTL peptide vaccine. Naïve female BALB/c mice (~4 wk old) were immunized on Day 0 and Day 7 by respiratory administration (50 μL IN) of vehicle alone (PBS), unencapsulated pp89-RR-EP67 (Free), or pp89-RR-EP67 encapsulated in ~5.4 μm PLGA 50:50 microparticles (MP) or ~350 nm PLGA 50:50 nanoparticles (NP) as described (Fig.1). Twenty-one days after immunization (Day 28), the average percent of pp89-responsive $CD8a^+$ cells ± SD (n=4 mice) in the (A) lungs and (B) spleen normalized to treatment with media alone was determined by ICS after incubating lymphocytes or splenocytes from each treatment group with media alone or media containing pp89 for 6 hrs then compared by ordinary one-way ANOVA with uncorrected Fisher's LSD test where $*P < 0.05$ and $**P < 0.01$. Data are representative of at least two independent experiments.

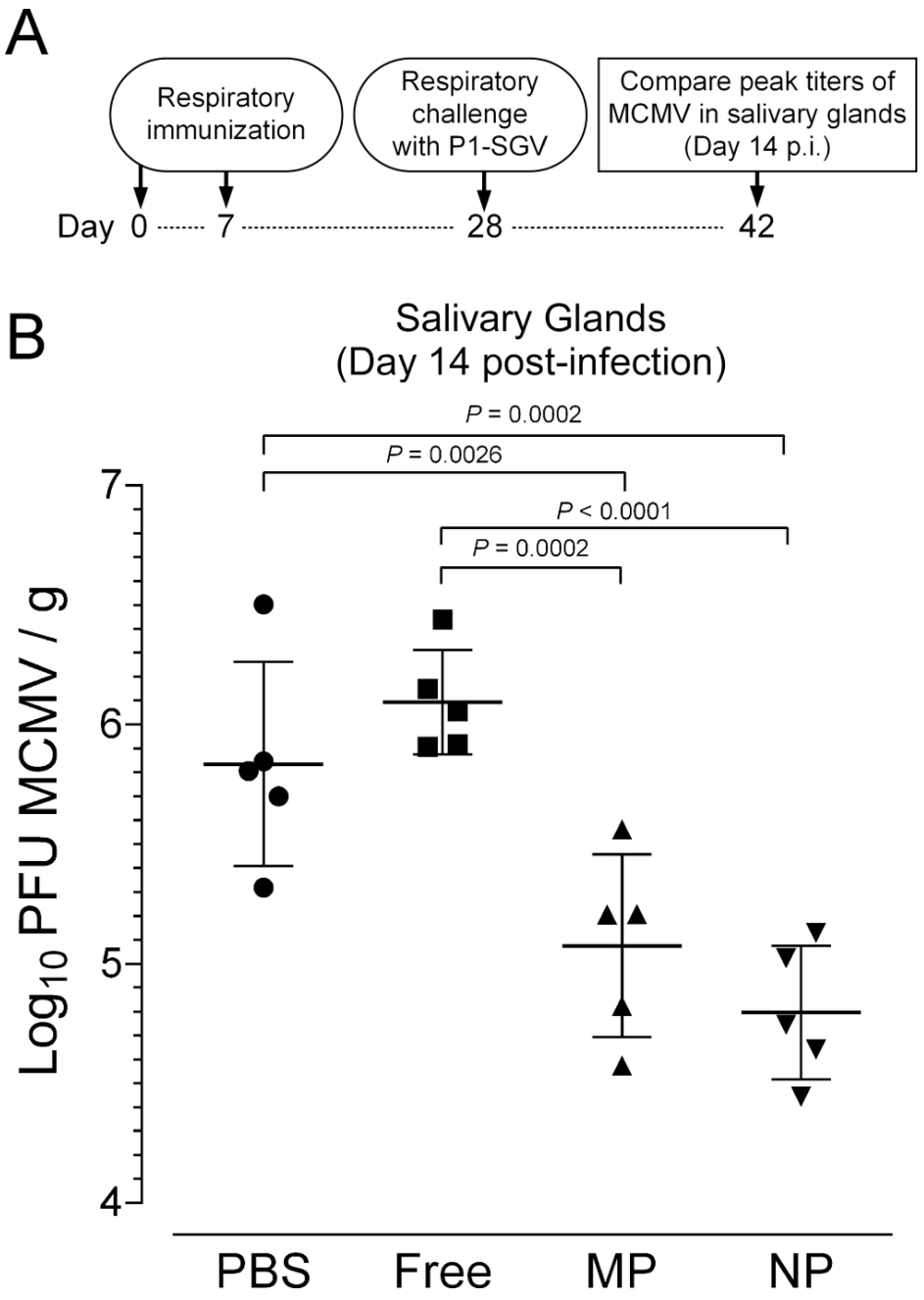

Figure 5.

The diameter of encapsulating biodegradable particle does not affect the relative efficacy of respiratory immunization with an EP67-conjugated CTL peptide vaccine against primary respiratory infection with MCMV. (A) Naïve female BALB/c mice (~4 wk old) were immunized on Day 0 and Day 7 by IN administration (50 μL) of vehicle alone (PBS), unencapsulated pp89-RR-EP67 (Free), or pp89-RR-EP67 encapsulated in ~5.4 μm PLGA 50:50 microparticles (MP) or ~350 nm PLGA 50:50 nanoparticles (NP) as described (Fig.1). Twenty-one days after the final immunization (Day 28), 5×10^4 PFU of salivary gland-derived MCMV passaged once in naïve BALB/c mice (P1-SGV) was administered in the

same manner as respiratory immunization and peak titers of productive MCMV in the salivary glands were compared (Day 42). (B) Average MCMV plaque forming units (Log_{10} PFU / g tissue ± SD) (n = 5 mice) in the salivary glands were determined on the day of peak infection by plaque assay against NIH/3T3 cells and compared by ordinary one-way ANOVA with uncorrected Fisher's LSD test. Data are representative of at least two independent experiments.

Table 1

Characteristics of pp89-RR-EP67-encapsulated PLGA 50:50 Microparticles and Nanoparticles.

Biodegradable Particles	Diameter (nm ± SD)	Loading (μg/mg ± SD)	EE% (± SD)	Zeta Potential (mv ± SD)	Burst Release (% loaded ± SD)
Microparticles (MP)	5402 ± 988	20 ± 4	43 ± 8	−22 ± 1	8 ± 2
Nanoparticles (NP)	350 ± 28	12 ± 2	25 ± 5	−12 ± 1	18.6 ± 0.3